

## General Disclaimer

### One or more of the Following Statements may affect this Document

- This document has been reproduced from the best copy furnished by the organizational source. It is being released in the interest of making available as much information as possible.
- This document may contain data, which exceeds the sheet parameters. It was furnished in this condition by the organizational source and is the best copy available.
- This document may contain tone-on-tone or color graphs, charts and/or pictures, which have been reproduced in black and white.
- This document is paginated as submitted by the original source.
- Portions of this document are not fully legible due to the historical nature of some of the material. However, it is the best reproduction available from the original submission.

**NASA TECHNICAL  
MEMORANDUM**

**NASA TM X-73482**

**NASA TM X-73482**

(NASA-TM-X-73482) MICROSTRUCTURE OF  
HOT-PRESSED  $Al_2O_3-Si_3N_4$  MIXTURES AS A  
FUNCTION OF HOLDING TEMPERATURE (NASA) 12 p  
HC \$3.50 CSCI 11D

N76-33287

Unclas  
05700  
G3/24

**MICROSTRUCTURE OF HOT-PRESSED  $Al_2O_3-Si_3N_4$  MIXTURES  
AS A FUNCTION OF HOLDING TEMPERATURE**

by Hun C. Yeh  
Lewis Research Center  
Cleveland, Ohio 44135

**TECHNICAL PAPER presented at the  
Sixth International Materials Symposium  
Berkeley, California, August 24-27, 1976**



MICROSTRUCTURE OF HOT-PRESSED  $\text{Al}_2\text{O}_3$ - $\text{Si}_3\text{N}_4$   
MIXTURES AS A FUNCTION OF HOLDING TEMPERATURE

Hun C. Yeh  
NASA Lewis Research Center/Cleveland State Univ.  
Cleveland, OH

ABSTRACT

Powder mixtures of 40 m/o  $\text{Si}_3\text{N}_4$ -60 m/o  $\text{Al}_2\text{O}_3$  were hot-pressed at 4000 psi at various holding temperatures from 1100°C to 1700°C. SEM and TEM results were correlated to X-ray phase analysis and density measurements. The progressively developed microstructure was used to interpretate the densification behavior of SIALON.

I. INTRODUCTION

In consolidation mixtures of  $\text{Si}_3\text{N}_4$  and  $\text{Al}_2\text{O}_3$  Wilson and Jack<sup>1</sup> and Oyama and Kamigaito<sup>2</sup> were the first to report, independently of each other, the existence of an expanded  $\beta$ - $\text{Si}_3\text{N}_4$  structure termed  $\beta'$  phase. This  $\beta'$  phase, first thought to be a solid solution of  $\text{Al}_2\text{O}_3$  in  $\beta$ - $\text{Si}_3\text{N}_4$ , has recently been determined to be a solid solution of  $\text{AlN}\cdot\text{Al}_2\text{O}_3$  in  $\beta$ - $\text{Si}_3\text{N}_4$ .<sup>3,4</sup> Dense bodies produced by hot pressing or pressureless sintering  $\text{Si}_3\text{N}_4$  and  $\text{Al}_2\text{O}_3$  consist primarily of  $\beta'$  and one or more minor phases. This type of material is now known as SIALON. SIALON, along with  $\text{Si}_3\text{N}_4$  and SiC, is a candidate for high temperature structural applications.

Dense SIALON reportedly has comparable mechanical properties and better corrosion resistance than that of  $\text{Si}_3\text{N}_4$ .<sup>1</sup> Initially the most attractive feature of this material was its higher sinterability than that of  $\text{Si}_3\text{N}_4$ , both with and without pressure during firing.<sup>1,5</sup> There were conflicting reports regarding the sinterability of SIALON without pressure (pressureless sintering).<sup>5,6</sup> The variety of results obtained were probably due to variations in impurity content and/or in the undisclosed additives. However, dense SIALON has been consolidated consistently by hot pressing without additives.

Despite the fact that dense SiALON bodies have been produced by hot pressing, very little information exists on the hot pressing behavior and mechanism of SiALON's. A recent study by Yeh et. al.<sup>7</sup> reported that at 1700°C no holding time was necessary to obtain a full dense body; that pore-free bodies were obtained at temperatures as low as 1550°C; and that phase transformation, solid solutioning and liquid phase formation were responsible for a high densification rate in the temperature range 1450°C - 1700°C. The present investigation is an extension of the above work, concentrating on microstructural studies. TEM and SEM results of a 60 m/o Al<sub>2</sub>O<sub>3</sub>-Si<sub>3</sub>N<sub>4</sub> powder mix hot-pressed for two hours at 1100°C, 1300°C, 1450°C, 1500°C, 1550°C, 1650°C, and 1700°C were correlated with x-ray phase analyses and end point densities. This study provides further information on the densification mechanism of SiALON's.

## II. EXPERIMENTAL PROCEDURES

### A) Materials

The starting materials were Plessey Frenchtown  $\alpha$ -Si<sub>3</sub>N<sub>4</sub> and Cabot ALON  $\gamma$ -Al<sub>2</sub>O<sub>3</sub> powders. The Si<sub>3</sub>N<sub>4</sub> powder was reported by the supplier to be 94%  $\alpha$  phase plus 6%  $\beta$  phase. In this study it was found to contain 0.92 w/o oxygen and 0.22 w/o carbon, 50 to 100 ppm calcium, 800 to 1200 ppm aluminum, and 300 to 500 ppm iron. The Al<sub>2</sub>O<sub>3</sub> powder was reported by the supplier to be essentially 100%  $\gamma$  phase and to have a metal impurity content of less than 0.1%. The morphology and size ranges of the as received powders were characterized in two dimensions by transmission electron microscopy. Plessey  $\alpha$ -Si<sub>3</sub>N<sub>4</sub> consists of fibrous and flake-like crystallites. The flakes range from 0.02 to 1.0 micrometer in the largest dimension and the fibers from 0.04 to 0.3 micrometer in width with a wide variation in length. The Al<sub>2</sub>O<sub>3</sub> powder particles are round and (according to the supplier) positively charged. Their size ranged from 0.005 to 0.09 micrometer, predominantly in the 0.01 to 0.02 micrometer range. The powders were mixed in a stirred steel ball mill as described in more detail in a previous report.<sup>7</sup> As a result the mixed powders contained approximately 0.6% Fe.

### B) Equipments And Procedures

A graphite vacuum hot press was used. A pressure of 27.6 MN/m<sup>2</sup> (4000 psi) was applied throughout the entire hot-pressing period, including the heat up and the holding period at temperature. Each hot-press run was heated to the desired temperature at the same rate (~19° C/min.) and was then followed by a two-hour hold. Fast cooling of the sample at the end of the hot

pressing run was accomplished by flushing the hot-press with He gas.

X-ray diffraction phase analysis of each sample was done on crushed powders of the sample using a diffractometer. TEM samples were prepared mechanically to an approximately sixty micrometer thick film, and then ion beam thinned to a thickness of the order of 1000Å. Scanning electron microscopy examination was made of fractured surfaces coated with vapor deposited gold. Scanning electron microscopy examination was also made on fractured specimens etched in HF for 24 hours at room temperature.

Density values were obtained by dividing the measured sample weight by the measured sample volume.

#### A) X-Ray Diffraction Analysis

Figure 1 shows the relative x-ray peak intensity of the phases present as a function of holding temperature.<sup>7</sup> It shows that there is no detectable interaction between  $\text{Si}_3\text{N}_4$  and  $\text{Al}_2\text{O}_3$  powder particles below 1300°C. Although the initial  $\gamma\text{-Al}_2\text{O}_3$  transforms to  $\alpha\text{-Al}_2\text{O}_3$ , the relative peak intensities of  $\text{Al}_2\text{O}_3$  and  $\text{Si}_3\text{N}_4$  remain unchanged. Above 1300°C,  $\beta'$  phase increases continuously while  $\alpha\text{-Al}_2\text{O}_3$  and  $\alpha\text{-Si}_3\text{N}_4$  decreases as the holding temperature increases. At 1500°C a new phase, termed X by Jack and Wilson<sup>1</sup>, appears and increases in the relative amount with temperature. Above 1650°C only  $\beta'$  and X phases are present. The interaction between  $\text{Al}_2\text{O}_3$  and  $\text{Si}_3\text{N}_4$ , accompanied by the increasing amount of  $\beta'$ , beginning at 1300°C, coincides with the onset of a fast rate of densification reported in a previous paper.<sup>7</sup> The appearance of X phase starting at 1500°C may also have enhanced the densification rate.<sup>7</sup>

#### B) Densities

End-point densities of samples hot-pressed for two hours at selected temperatures are shown in Fig. 2. A scale in terms of percent of the density of the 1700°C sample is shown on the right-hand side of the figure. The indicated phases present in the sample were taken from Fig. 1 to provide a reference for discussion. The 1550°C, 1650°C, and 1700°C samples are all pore-free. The reason for the 1550°C sample having a higher density than that of the 1700°C sample is the presence of unreacted  $\alpha\text{-Al}_2\text{O}_3$  which is higher in density than  $\text{Si}_3\text{N}_4$ .

#### C) Transmission Electron Microscopy

Figure 3 (parts "a" through "b") shows transmission electron micrographs of samples hot-pressed at temperatures ranging from 1300° to 1650°C. The 1100°C sample is too porous to make a good TEM sample. These microstructures will be discussed

with reference to the x-ray and density results presented in sections III (A) and (B).

From the X-ray results, at 1300°C and below,  $\text{Al}_2\text{O}_3$  and  $\text{Si}_3\text{N}_4$  powder crystallites did not interact with each other. However a 6% increase in density (Fig. 2) occurred in the 1300°C specimen as compared with the 1100°C specimen. This density increase has been attributed to the compaction of  $\text{Al}_2\text{O}_3$ .<sup>7</sup> It is now clearly seen in Fig. 3a that there are regions of the sample, such as the area near the center of the micrograph, where the fine grained equiaxed structure is compacted  $\text{Al}_2\text{O}_3$ . The flaky crystallites are undoubtedly  $\text{Si}_3\text{N}_4$ . Voids are abundant, in agreement with the fact the bulk density is only 58% of the 1700°C specimen (Fig. 2).

At 1450°C (Fig. 3b) most of the flaky crystallites ( $\text{Si}_3\text{N}_4$ ) and equiaxed fine grains ( $\text{Al}_2\text{O}_3$ ) disappear. The extensive interaction between the two constituents caused the change in grain morphology. The interaction is also evident in the x-ray results. The variations in shade within some grains may suggest inhomogeneity in composition. Also grain boundaries are not well defined. These two observations indicate that the reaction were not completed. Referring to x-ray data in Fig. 1,  $\alpha$ - $\text{Al}_2\text{O}_3$  S.S.,  $\alpha$ - $\text{Si}_3\text{N}_4$  S.S., and  $\beta'$  are all present at about the same amount.

At 1500°C (Fig. 3c), the number of voids is drastically reduced. Grain boundaries are better defined and the shade within each grain is more uniform. A new morphological feature is the small white dots ( $\sim 300\text{\AA}$  in size) within the grains, some with hexagonal shape. These dots were identified as voids distributed through the thickness of the thin film specimen by TEM stage tilting and stereomicrograph techniques. A dark rounded phase is also seen. There is still some portion of the sample which is an aggregate of fine  $\text{Al}_2\text{O}_3$  grains. No dislocations are seen, suggesting that there was no plastic deformation during hot-pressing up to this temperature. A few grains with typical grain boundary fingers are evident, indicating equilibrium grain boundaries.

At 1550°C (Fig. 3d) the microstructure is similar to that at 1500°C except that the aggregates of fine  $\text{Al}_2\text{O}_3$  grains have been reduced to a minimum. The grains have grown larger and more equiaxed compared with those at 1500°C. Some grains with striations are also present. According to Lewis and Drews<sup>9</sup>, the striations are anti-phase-boundary faults and/or twins which are characteristics of X phase grains. If the melting point of X phase proposed by Layden<sup>3</sup>,  $\sim 1650^\circ\text{C}$ , is a good estimation then the X phase observed in Fig. 3d formed by a solid state reaction. The presence of X phase at 1550°C is supported by the x-ray results (Fig. 1).

At 1650°C (Fig. 3e) no fine-grained  $\text{Al}_2\text{O}_3$  is found in the microstructure, but more striated grains are found indicating an increased amount of X phase. The striated grains were

liquid at one time, if the melting point ( $\sim 1650^{\circ}\text{C}$ ) for X phase proposed by Layden<sup>3</sup> is correct. The black rounded phase and the white dots (voids) have both greatly diminished. The bulk of the sample is composed of equiaxed grains with uniform shade which is undoubtedly  $\beta'$  phase. More grains have boundary fingers and more grains are faceted, indicating an equilibrium grain structure after grain growth. No apparent evidence of dislocations is found. No flake-like or fibrous crystallite grain morphology (the morphology of the starting  $\text{Si}_3\text{N}_4$  powder) is retained in this fully dense body. The microstructure of the  $1700^{\circ}\text{C}$  sample is essentially identical to that of  $1650^{\circ}\text{C}$ , and therefore is not shown.

#### D) Scanning Electron Microscopy

Scanning electron microscopy was used because it can reveal the structure of a very porous body, the three dimensional grain (or crystallite) morphology, and the fracture mode. Figure 4 (parts "a" through "e") shows fractured surfaces of some selected samples hot-pressed in the temperature range under investigation. Notice the drastic change in structure as the hot pressing temperature increases.

Fig. 4a is the SEM micrograph of the fractured surface of the  $1100^{\circ}\text{C}$  sample. Large voids (1 to 2  $\mu\text{m}$ ) as well as smaller pores (0.1  $\mu\text{m}$ ) are present in the micrograph. Fine particles on the order of 0.2  $\mu\text{m}$  size are seen throughout the fractured surface based on knowledge of the morphology and size of the starting  $\text{Al}_2\text{O}_3$  particles (spherical and 0.02  $\mu\text{m}$ ) respectively. The fine particles are believed to be conglomerates of  $\text{Al}_2\text{O}_3$  particles. These finer conglomerates which surround and adhere to the larger  $\text{Si}_3\text{N}_4$  crystallites are the matrix in the powder compact. The presence of the individual  $\text{Al}_2\text{O}_3$  conglomerates would indicate that very little, if any, densification had occurred in the  $\text{Al}_3\text{O}_4$  matrix. This is why there is only a two percent increase in density as compared with the green compact (Fig. 2). Therefore Fig. 4a is essentially the structure of a green compact.

At  $1300^{\circ}\text{C}$  (Fig. 4b) the amount of voids is significantly reduced, as reflected in a larger increase in density (Fig. 2). Fine spherical  $\text{Al}_2\text{O}_3$  particles had compacted (sintered) to form crystalline aggregates (also see fine-grained regions in Fig. 3a). As a result,  $\text{Si}_3\text{N}_4$  crystallites, which have the characteristic fibrous (or rod like) and flaky morphologies, are no longer obscured by the fine  $\text{Al}_2\text{O}_3$  and are exposed in the fractured surface. Some isolated fine spherical  $\text{Al}_2\text{O}_3$  particles are still visible. No attempt is made to differentiate the large  $\text{Al}_2\text{O}_3$  crystallites from  $\text{Si}_3\text{N}_4$  crystallites.

At  $1450^{\circ}\text{C}$  (Fig. 4c) the crystallites are rounded and more agglomerated, indicating a significant degree of diffusion-

controlled interaction between crystallites. This observation is in agreement with the x-ray results (Fig. 1) at this temperature. The increased interaction between crystallites is also evident in the TEM micrographs by comparing the degree of intergranular bonding in Fig. 3a and Fig. 3b.

When the hot pressing temperature was increased to 1550°C a pore-free structure is obtained (Fig. 4d). The outline of grains/crystallites on the fractured surface is less defined; this may be attributed to the extensive diffusion-controlled reaction between grains/crystallites and the formation of X phase, both of which occurred at this temperature as shown in the x-ray data (Fig. 1). The rounded grain morphology observed by TEM on the same sample (Fig. 3c) is in agreement with the above observation.

When the hot pressing temperature was increased to 1700°C, the structure of the fractured surface is almost featureless (Fig. 4e). This unusual structure prompted the investigator to etch the fractured surface of this sample, as well as other samples discussed in this section, to obtain additional information (see the next sub-section).

#### A) Scanning Electron Microscopy Of HF Etched Samples

Samples hot-pressed at 1100°, 1300°, 1450°, 1550°, and 1700°C respectively were chosen for the etching study. Fractured samples were immersed in HF for 24 hours at room temperature and then cleaned by rinsing with distilled water and alcohol.

No detectable difference was found for the 1100°, 1300°, and 1450°C samples before and after etching. However, etching did reveal a drastically different structure for both the 1550°C and 1700°C samples (Fig. 5) as compared with the unetched specimen (Figs. 4d&e). Apparently one or more phases had been etched away. To identify the etched phase, x-ray powder specimens were ground off from the same face of the sample before and after etching. The results showed that X phase was the only phase which was etched away in both 1550° and 1700°C samples. The amount of voids seen in the etched specimens far exceeds the amount of X phase detected by x-ray phase analysis and TEM results (Figs. 1 and 3) presented earlier, particularly in the 1550°C sample. It is believed that X phase is interlocked with the other phase (s) present in the specimen. As a result of the removal of X phase in etching, other unetched grains were dislodged or carried away during etching and/or cleaning of the specimen before SEM examination.

Figure 5 shows that the crystallites/grains remaining after etching are mostly equiaxed. The  $\beta'$  phase grains are better defined and larger in size in the 1700°C sample than grains in the 1550°C sample.



#### IV. DISCUSSION AND CONCLUSION

Plastic deformation, particle fragmentation, particle rearrangement and pressure-enhanced diffusion are some of the models (or mechanisms) proposed to explain the densification of single-phase systems under hot-pressing<sup>9</sup>. A multiphase system, such as the one investigated in the paper, will undoubtedly permit additional densification mechanisms.

The results presented in section III show that densification of hot-pressed SiAlON did not involve detectable amounts of plastic deformation (almost no dislocations were observed). The major densification mechanisms were diffusion-controlled reactions which resulted in the formation of a new phase, the disappearing of an old one, solid solutioning and the liquid phase formation. The above diffusion-controlled phenomena were believed to be enhanced by the applied pressure during hot pressing. The enhancement could be a combination of a reduction in reaction energy and better contact and shorter diffusion paths. A cold pressed powder compact, prepared identically to those used for hot-pressing, did not densify when held without pressure at 1700°C for two hours in nitrogen atmosphere. Other than the skin layer of the sample which decomposed at high temperature, the sample consisted of primarily  $\mu$  and X phases, similar to the hot-pressed one.

In summary, the microstructure results show that in hot-pressing a 60 m/o  $\text{Al}_2\text{O}_3\text{-Si}_3\text{N}_4$  powder mix the following phenomena (or mechanisms) took place as the holding temperature was increased.

- (1) Room Temperature- 1100°C: Particle rearrangement and fragmentation.
- (2) 1100° - 1300°C: Consolidation of  $\text{Al}_2\text{O}_3$  particles to larger crystalline aggregates
- (3) 1300° - 1500°C: Pressure enhanced, diffusion controlled reactions resulting in solid solutioning and  $\alpha \rightarrow \beta\text{-Si}_3\text{N}_4$  transformation
- (4) 1500° - 1550°C: X phase was formed in addition to the phenomena occurring in 1300° - 1500°C.
- (5) 1550° - 1700°C: The formation of a liquid (X phase composition). A liquid solution/recrystallization<sup>8</sup> through the molten X phase followed by grain growth was responsible for the fully dense body with equiaxed structure (Fig. 3e).

#### ACKNOWLEDGEMENTS

The writer thanks Drs. R. L. Ashbrook, H. B. Probst, and T. P. Herbell for valuable discussions.

## REFERENCES

1. K. H. Jack and W. I. Wilson: "Ceramics Based on the Si-Al-O-N and Related Systems," *Nature Physical Science*, 238 (July 10, 1972), pp. 28-29.
2. Y. Oyama and O. Kamigaito: "Hot-Pressing of  $\text{Si}_3\text{N}_4\text{-Al}_2\text{O}_3$ ." *Journal of Ceramic Society of Japan* 80, 8 (1972), pp. 327-336.
3. G. K. Layden: "Process Development for Pressureless Sintering of SiAlON Ceramic Components," Final Report, Contract N00019-75-0232, Naval Air System Command, Feb., 1976.
4. L. J. Gauckler, H. L. Lukas and A. G. Petzow: "Contribution To the Phase Diagram  $\text{Si}_3\text{N}_4\text{-AlN-Al}_2\text{O}_3\text{-SiO}_2$ ," *J. Am. Ceramic Soc.*, Vol. 58, No. 7-8, 1975.
5. W. J. Arrol: "The Sialons-Properties and Fabrication" Chapter 34 in *Ceramics for High-Performance Applications*, Proceedings of the Second Army Materials Technology Conference, Hyannis Massachusetts, November 1973, Brook Hill Publishing Company, 1974.
6. F. F. Lange: "Fabrication and Properties of Silicon Compounds - Task I. Fabrication Microstructure and Selected Properties of SiAlON Compositions," Westinghouse Electric Corporation Research Laboratories Naval Air Systems Command, Final Report, Contract N00019-73-C-0208, Feb. 26, 1974.
7. H. C. Yeh, W. A. Sanders and J. L. Fiyako: "Pressing Sintering of SiAlON's" Accepted for publication in *Am. Ceramic Soc. Bulletin*, Nov. 1976.
8. P. Drew and M. H. Lewis: "The Microstructures of Silicon Nitride/Alumina Ceramics." *J. Mat. Sci.*, 9 (1974) 1833-1838.
9. R. M. Spriggs and L. Atteraaas: "Densification of Single-Phase Systems Under Pressure," *Ceramic Microstructure*, edited by R. M. Fultrath and J. A. Pask, John Wiley, 1968.

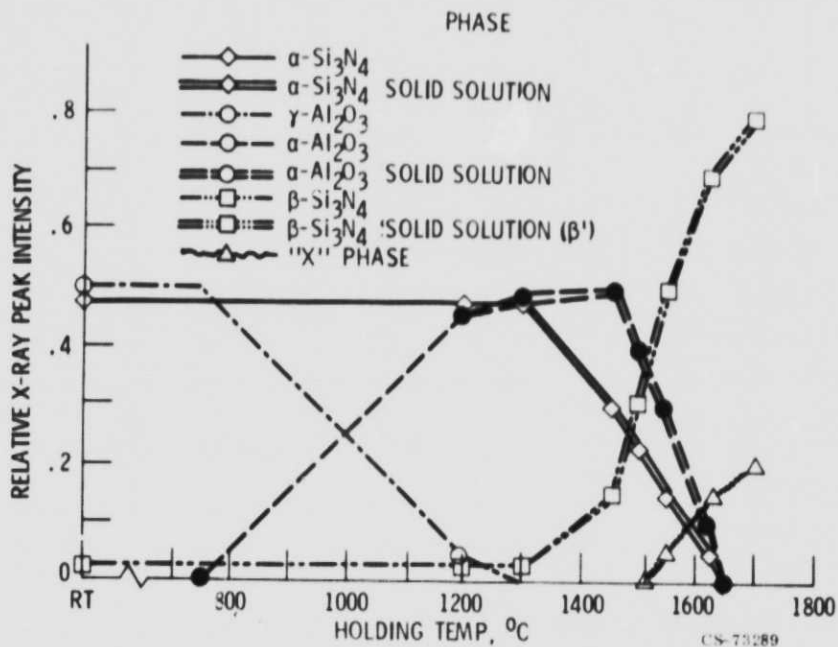


Figure 1. - Relative X-ray peak intensities for phases present in 40-mol %  $\text{Si}_3\text{N}_4$  - 60-mol %  $\text{Al}_2\text{O}_3$  powder compacts after pressure sintering followed by 2-hour holding period at temperature to 1700° C (3090° F).

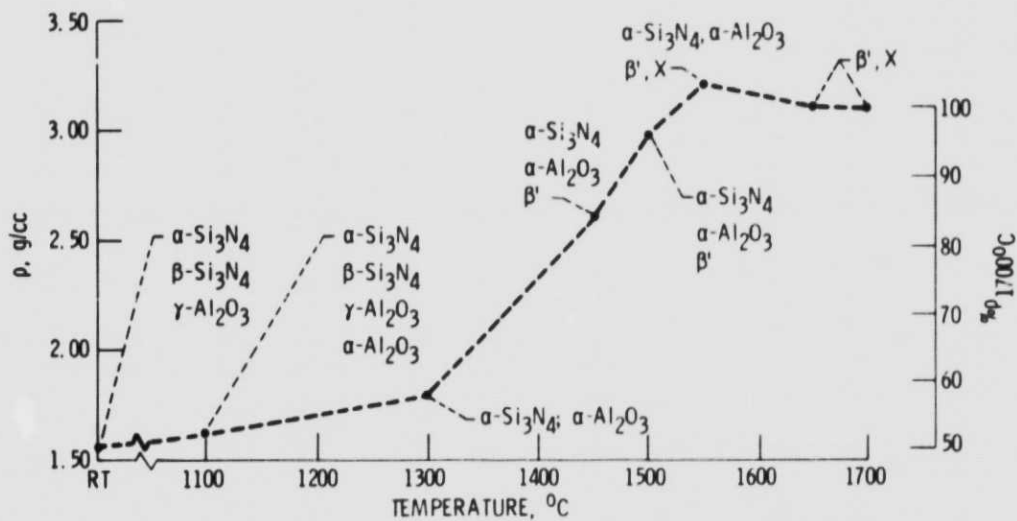
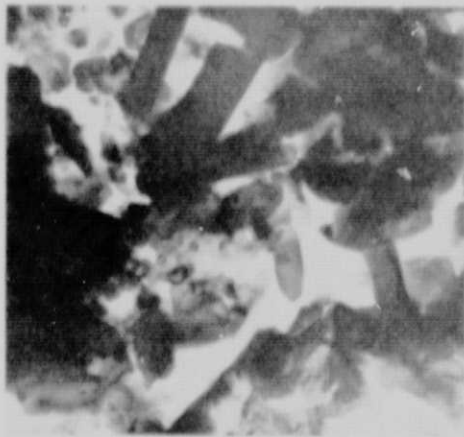
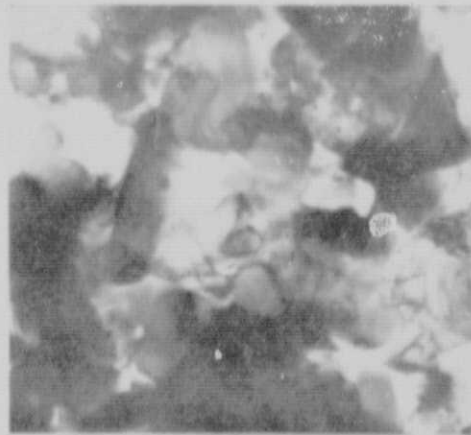


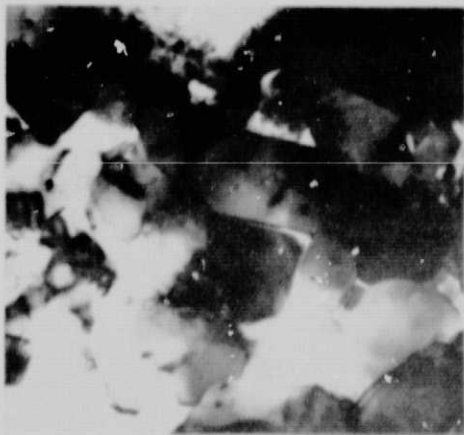
Figure 2. - Density versus pressing temperature of 60 m/o  $\text{Al}_2\text{O}_3$ - $\text{Si}_3\text{N}_4$  powder compacts after vacuum hot-pressing at 27.6 MN/m<sup>2</sup> (4000 psi) - 2 hours, with phases present indicated.  $\% \rho_{1700^\circ\text{C}}$  is percent of density of the 1700° C specimen.



(a) 1300° C.



(b) 1450° C.



(c) 1500° C.



(d) 1550° C.



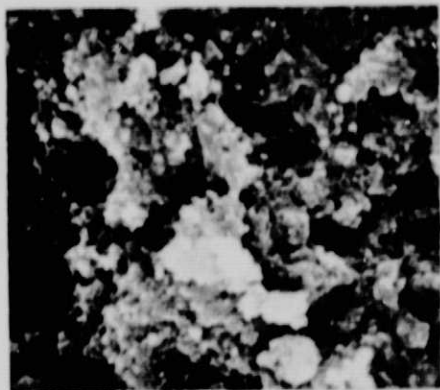
(e) 1650° C.

Figure 3. - Transmission electron micrographs of 60 m/o  $\text{Al}_2\text{O}_3\text{-Si}_3\text{N}_4$  powder compacts after vacuum hot-pressing at  $27.6 \text{ MN/m}^2$  (4000 psi) for two hours at the indicated temperatures

CS-77556

ORIGINAL PAGE IS  
OF POOR QUALITY

E-8865



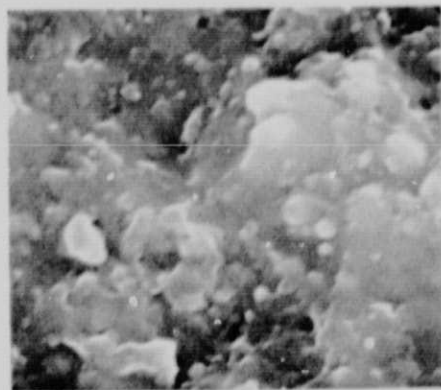
(a) 1100° C.



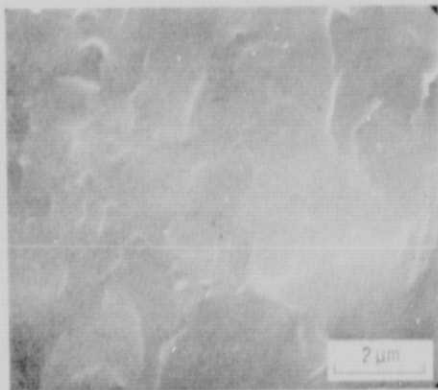
(b) 1300° C.



(c) 1450° C.



(d) 1550° C.



(e) 1700° C.

Figure 4. - Scanning electron micrographs of fractured surfaces of 60 m/o  $\text{Al}_2\text{O}_3\text{-Si}_3\text{N}_4$  powder compacts after vacuum hot-pressing at  $27.6 \text{ MN/m}^2$  (4000 psi) for two hours at the indicated temperatures.

CS-77557

ORIGINAL PAGE IS  
OF POOR QUALITY



(a) 1550<sup>o</sup> C.



(b) 1700<sup>o</sup> C.

Figure 5. Scanning electron micrographs of etched fractured surfaces (24 hours in HF at room temperature) of 60 m/o  $\text{Al}_2\text{O}_3\text{-Si}_3\text{N}_4$  powder compacts after vacuum hot-pressed at  $27.6 \text{ MN/m}^2$  (4000 p.s.i.) for two hours at the indicated temperatures.

CS-77555